



Providing Choice & Value

Generic CT and MRI Contrast Agents



CONTACT REP

AJNR

This information is current as
of July 23, 2025.

**Percutaneous CT-Guided Core Needle
Biopsies of Head and Neck Masses: Review of
184 Cases at a Single Academic Institution,
Common and Special Techniques, Diagnostic
Yield, and Safety**

R.W. Jordan, D.P. Shlapak, J.C. Benson, F.E. Diehn, D.K.
Kim, V.T. Lehman, G.B. Liebo, A.A. Madhavan, J.M.
Morris, P.P. Morris, J.T. Verdoorn and C.M. Carr

AJNR Am J Neuroradiol 2022, 43 (1) 117-124

doi: <https://doi.org/10.3174/ajnr.A7348>

<http://www.ajnr.org/content/43/1/117>

Percutaneous CT-Guided Core Needle Biopsies of Head and Neck Masses: Review of 184 Cases at a Single Academic Institution, Common and Special Techniques, Diagnostic Yield, and Safety

 R.W. Jordan,  D.P. Shlapak,  J.C. Benson,  F.E. Diehn,  D.K. Kim,  V.T. Lehman,  G.B. Liebo,  A.A. Madhavan,  J.M. Morris,  P.P. Morris,  J.T. Verdoorn, and  C.M. Carr



ABSTRACT

BACKGROUND AND PURPOSE: Percutaneous CT-guided core needle biopsies of head and neck lesions can be safely performed with vigilant planning. This largest-to-date single-center retrospective study evaluates multiple approaches with consideration of special techniques and examines the histopathologic yield.

MATERIALS AND METHODS: Retrospective review of CT-guided core biopsies of head and neck lesions from January 1, 2010, to October 30, 2020, was performed. We recorded the following: patient demographics, sedation details, biopsy needle type and size, lesion location and size, approach, patient positioning, preprocedural intravenous contrast, proceduralists' years of experience, complications, and pathology results.

RESULTS: One hundred eighty-four CT-guided core biopsies were evaluated. The initial diagnostic yield was 93% (171/184). However, of 43/184 (23%) originally "negative for malignancy" biopsies, 4 were eventually positive for malignancy via rebiopsy/excision, resulting in a 2% false-negative rate and an adjusted total diagnostic yield of 167/184 (91%). Biopsies were performed by 16 neuroradiologists with variable experience. The diagnostic yield was essentially the same: 91% (64/70) for proceduralists with ≤ 3 years' experience, and 90% (103/114) with > 3 years' experience. The diagnostic yield was 93% (155/166) for lesions of > 10 mm. The diagnostic yield per biopsy needle gauge was the following: 20 ga, 81% (13/16); 18 ga, 93% (70/75); 16 ga, 90% (64/71); and 14 ga, 91% (20/22). There were 4 asymptomatic hematomas, with none requiring intervention.

CONCLUSIONS: Percutaneous CT-guided core needle biopsies are safe procedures for superficial and deep head and neck lesions with a high diagnostic yield. Careful planning and special techniques may increase the number of lesions accessible percutaneously while minimizing the risk of complications.

ABBREVIATIONS: CNB = core needle biopsy; FNA = fine-needle aspiration; H&N = head and neck; SCC = squamous cell carcinoma

An estimated $> 54,000$ new cases of oral cavity and pharyngeal cancer and 44,280 new cases of thyroid cancer will be diagnosed in the United States in 2021, not including head and neck (H&N) lymphomas, salivary gland tumors, and other less common malignancies.¹

If not apparent on direct visualization, H&N lesions often require image-guided biopsy. Prior studies have shown higher

diagnostic yields of image-guided core needle biopsy (CNB) versus fine-needle aspiration (FNA), including parotid, submandibular, and sublingual gland lesions, as well as cervical lymphadenopathy.²⁻⁵ Additionally, supplementary FNA during lymph node CNB might not contribute to an actionable diagnosis in cases of lymphoma.⁶


Several standard approaches to H&N CT-guided CNB are used, including subzygomatic, paramaxillary, retromandibular, anterior, lateral, and posterior approaches.⁷⁻¹³ These are illustrated in Fig 1. A recently published review of 27 CT-guided CNBs by Hillen et al¹⁴ demonstrated the effectiveness and safety of these procedures for H&N lesions. However, large studies evaluating the diagnostic yield and safety profile of CT-guided H&N CNBs with a variety of locations and lesion sizes are lacking. In this study, we sought to review and describe our institution's experience with CT-guided CNB of H&N lesions, with emphasis on the diagnostic

Received June 11, 2021; accepted after revision September 14.

From the Division of Neuroradiology, Department of Radiology, Mayo Clinic, Rochester, Minnesota.

Paper was previously presented at a scientific presentation at: Annual Meeting of the American Society of Head & Neck Radiology, September 8–12, 2021; Virtual.

Please address correspondence to Darya Shlapak, MD, Department of Radiology, Mayo Clinic, 200 First St SW, Rochester, MN 55905; e-mail: Shlapak.darya@mayo.edu

 Indicates article with online supplemental data.

<http://dx.doi.org/10.3174/ajnr.A7348>

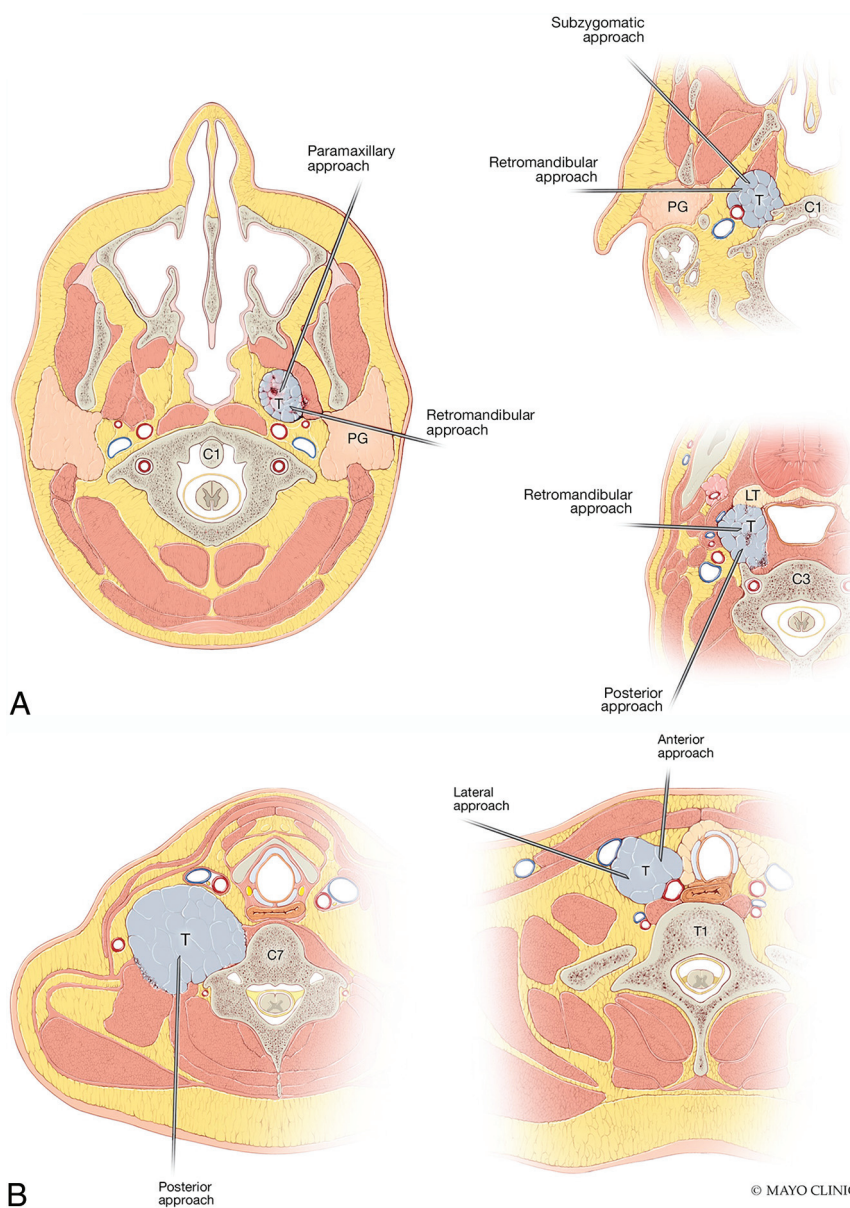


FIG 1. Common biopsy approaches to H&N lesions at different levels of the suprahyoid (**A**) and infrahyoid neck (**B**). Note that to avoid the parotid gland, one should use a retromandibular approach for more inferior retropharyngeal, parapharyngeal, pharyngeal mucosal, and masticator space lesions; more superior lesions are better accessed via paramaxillary and subzygomatic approaches. Reprinted with permission of Mayo Foundation for Medical Education and Research, all rights reserved. PG indicates parotid gland; T, tumor; LT, lingual tonsil.

and histopathologic yields and attention to target lesion and needle-gauge size, approach, safety profile, and special techniques.

MATERIALS AND METHODS

Patient Selection and Enrollment

This was a Health Insurance Portability and Accountability Act-compliant retrospective study, approved by the institutional review board. Informed consent was waived.

Our radiologic database was searched to identify all CT-guided H&N biopsies from January 1, 2010, to October 30, 2020. Search

terms including “CT biopsy,” “CT-guided biopsy,” and “CT neuro biopsy” were autopopulated in our reporting template. This search yielded 1211 results. Inclusion criteria were biopsy with CT guidance, core biopsy, and location in the H&N. Biopsies outside the H&N (including the calvaria and spine) and FNAs were excluded. Ultimately, 184 core biopsies from 174 patients were included in the final study cohort.

Imaging and Clinical Review

Intraprocedural CT images, procedure reports, clinical follow-up notes, and pathology reports were reviewed by a neuroradiology fellow. For each biopsy case, the following data were collected (if available): patient demographics, biopsy needle gauge and brand, sedation type, biopsy approach, gantry tilt, patient positioning, anatomic space of the target lesion, maximal dimension of the lesion in the axial plane, proceduralists’ years of experience, administration of pre- and intraprocedural contrast, histopathology, and complications. Intraprocedural CT images, reports, and the next patient encounter were reviewed for evaluation of procedure-related complications.

CT Imaging Parameters

A standard optimized dose protocol was used for all CT-guided core biopsies, using spiral CT with 1-second rotation time, 0.9 pitch, 120 kV(peak), 130 mAs, with an average volume CT dose index of 17.52 mGy for the planning phase. For the actual biopsy i-Sequence, 3 or 6 slices were used with 2.4- or 4.8-mm section thickness per the proceduralist’s preference, with a 0.5-second rotation time, 120 kVp, 80 versus 40 mAs, and a CT dose index of 8.28 versus 4.14 mGy per scan, respectively (2.4- versus

4.8- mm section). Reduced dose protocols were used in the pediatric population. Preprocedural CT with contrast when necessary was performed according to routine neck CTA or CT soft-tissue neck protocol with iohexol contrast (Omnipaque 350 or Omnipaque 300; GE Healthcare) and “trigger of aorta,” and 80-second delay, respectively.

Special Techniques

Preprocedural and Intraprocedural IV Contrast. The use of IV contrast is not uncommon for deep H&N biopsies and allows planning the safest approach to avoid major vascular structures (Fig 2A–F and Fig 3D). Additionally, IV contrast can make the

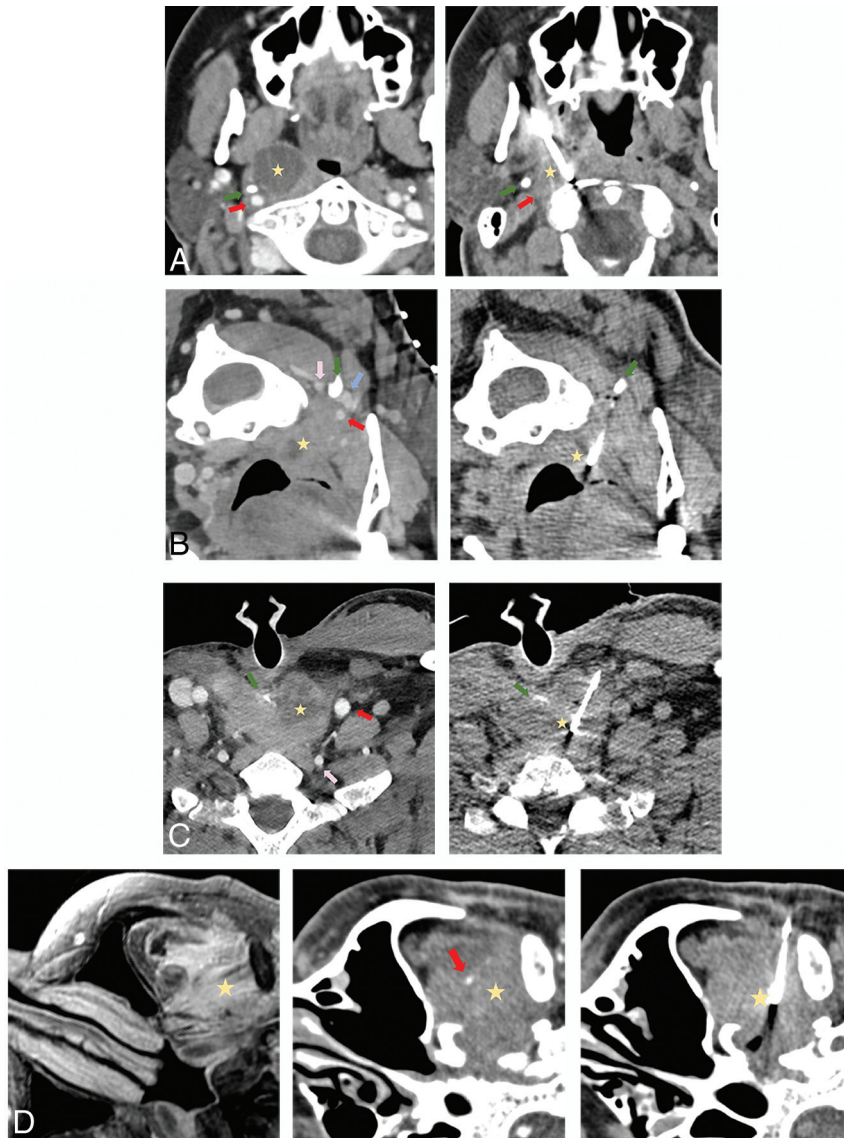


FIG 2. Common approaches used in the current series biopsy. **A**, A paramaxillary approach targeting a 1.9-cm partially cystic right retropharyngeal lymph node (yellow star). *Left*, Preprocedural contrast-enhanced CT (venous phase) to better visualize the right ICA (red arrow) and better assess lesion margins due to peripheral enhancement. *Right*, Intraprocedural CT with a 14-ga needle through the lesion (part of the cystic component was initially aspirated). The styloid process (green arrow) is a useful landmark because it is immediately anterior to the ICA. Recurrent human papillomavirus (HPV) + SCC. This approach is commonly used to access retropharyngeal, parapharyngeal, pharyngeal mucosal, masticator, and deep parotid space lesions. **B**, A retromandibular approach in a patient in a prone position targeting a 1.1-cm partially cystic left retropharyngeal lymph node (yellow star). *Left*, Contrast-enhanced CT (venous phase) to better visualize the left ICA (red arrow), vertebral artery (pink arrow), and internal jugular (IJ) vein (blue arrow) and highlight more solid lesion portions. *Right*, Intraprocedural CT with a 16-ga needle through the solid portion of the lesion. The C1 transverse process (green arrow) is a useful landmark because it “marks a safe pass” between the vertebral artery posterior to the needle and the ICA/IJ vein anteriorly. Recurrent HPV + SCC. This approach can be used for more inferior retropharyngeal, parapharyngeal, pharyngeal mucosal, masticator, and deep parotid lesions, as well as sublingual, submandibular, perivertebral, and carotid space lesions. **C**, Anterior approach targeting a 3.4-cm partially cystic nodule at the tracheoesophageal groove (yellow star). *Left*, Preprocedural contrast-enhanced CT (venous phase) to opacify the left common carotid artery (red arrow) and vertebral artery (pink arrow) and delineate the solid component of the target lesion. *Right*, Intraprocedural CT with an 18-ga needle through the solid component of the lesion. A partially visualized esophageal stent (green arrow) is a useful landmark showing the approximate location of the infiltrated esophagus, lateral to the stent. Recurrent SCC. This approach is used with a neutral supine position for more midline anterior neck lesions such as the visceral space, level VI, and the supraclavicular lymph nodes. **D**, A subzygomatic approach targeting an infiltrating left masticator space mass seen on MR imaging (left image, yellow star). *Middle*, Preprocedural contrast-enhanced CT (venous phase) to opacify the left internal maxillary artery (red arrow). *Right*, Intraprocedural CT with an 18-ga needle through the infiltrating lesion with the biopsy device clearly posterior to the expected location of the internal maxillary artery in correlation with the middle image. Recurrent SCC with perineural spread. By far, masticator space lesions are the most common targets for this approach.

lesion more conspicuous and help direct the biopsy toward more solid components of a cystic/necrotic mass, potentially increasing the diagnostic yield (Fig 2B, -C, and -F).

To our knowledge, the use of intraprocedural contrast during H&N lesion core sampling has not been reported, though intraprocedural contrast-enhanced CT was recently described for the

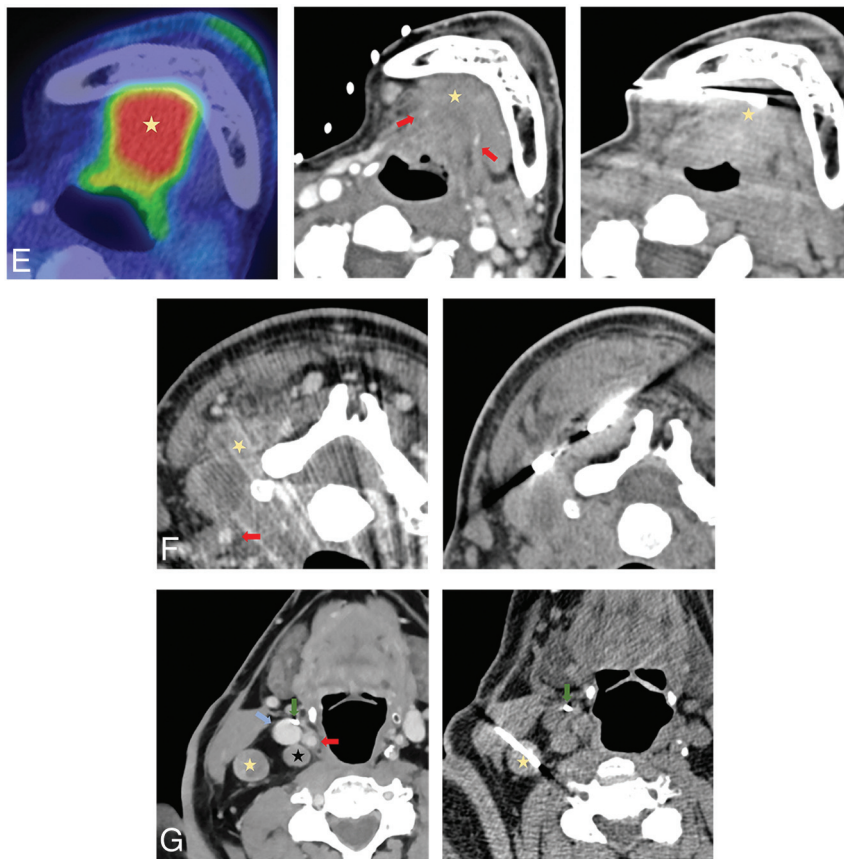


FIG 2. Continued E, Submandibular approach targeting diffuse soft-tissue thickening in the sublingual space, hypermetabolic on PET/CT (*left image*, yellow star). *Middle*, Preprocedural contrast-enhanced CT (venous phase) to localize and avoid vascular structures (*red arrows*). *Right*, Intraprocedural CT with an 8-ga needle trough through the lesion with the biopsy device clearly anterior to the expected location of the prominent vessels in correlation with the middle image. Adenoid cystic carcinoma. This approach offers access to the sublingual and submandibular spaces, level IA and IB lymph nodes, and potentially retropharyngeal/parapharyngeal lesions; however, it would require gantry tilt and/or neck manipulation. **F**, Posterior approach with the patient in a prone position targeting the more posterior component of the bilobed 5.3-cm partially cystic mass in the left perivertebral space. *Left*, Preprocedural contrast-enhanced CT (venous phase) to localize the ICA (*red arrow*) and delineate solid components of the mass (*yellow star*). *Right*, Intraprocedural CT with a 14-ga needle trough through the solid portion of the lesion. Metastatic papillary thyroid carcinoma. Perivertebral and carotid space lesions and level V lymph nodes are most accessible with this approach, usually with the patient in a prone position. **G**, A lateral approach targeting a right-level IIB 1.5-cm lymph node seen on the routine contrast-enhanced soft-tissue neck CT (*left image*, yellow star). Preprocedural contrast was not obtained because prior soft-tissue neck CT (*left image*) showed that the ICA (*red arrow*) and the IJ vein (*blue arrow*) can be well-visualized with at least a 7-mm fat plane between vessels and target lesion. Note the postoperative right carotid endarterectomy clip (*green arrow*) and an additional smaller metastatic lymph node (*black star*) too close to the vessels. *Right*, Intraprocedural CT with a 16-ga needle trough through the target. Metastatic small-cell carcinoma. This approach is commonly used to access levels II–IV and sometimes level V and the supraclavicular lymph nodes.

evaluation of the completeness of renal mass ablation.¹⁵ While this is not a standardized technique at our institution, depending on the proximity of the critical vascular structure to the target lesion, proceduralists can choose to slowly infuse IV contrast during lesion sampling to continuously opacify and visualize adjacent vessels (Fig 4).

Gantry Tilt and/or Neck Flexion/Extension. Modern CT scanners allow gantry tilting to provide variable degrees of angle access to approach deep lesions while bypassing vascular and osseous structures, which otherwise would be difficult to avoid. Neck flexion/extension can partially compensate for gantry tilt because steep gantry tilt considerably narrows the working space for the proceduralist within the CT scanner bore (Fig 3C).

RESULTS

Patient Demographics and Periprocedural Details

One hundred seventy-four patients with 184 CT-guided CNB procedures were included in the final cohort. Eight patients underwent 2 biopsies, and 1 patient, 3 biopsies. The mean patient age at the time of the biopsy was 60 years (range, 2–86 years); 70 (38%) were female. All procedures were performed by a total of 16 board-certified and board-eligible fellowship-trained neuroradiologists. A trainee (resident or fellow) assisted in 95/184 (52%) cases.

Moderate sedation was administered in 145 cases (79%); general anesthesia, in 23 cases (13%); and only local anesthetic, in 16 cases (7%). A 14-ga core biopsy needle was used in 22 cases (12%); 16 ga, in 71 cases (39%); 18 ga, in 75 cases (41%); and 20 ga, in 16 cases (9%).

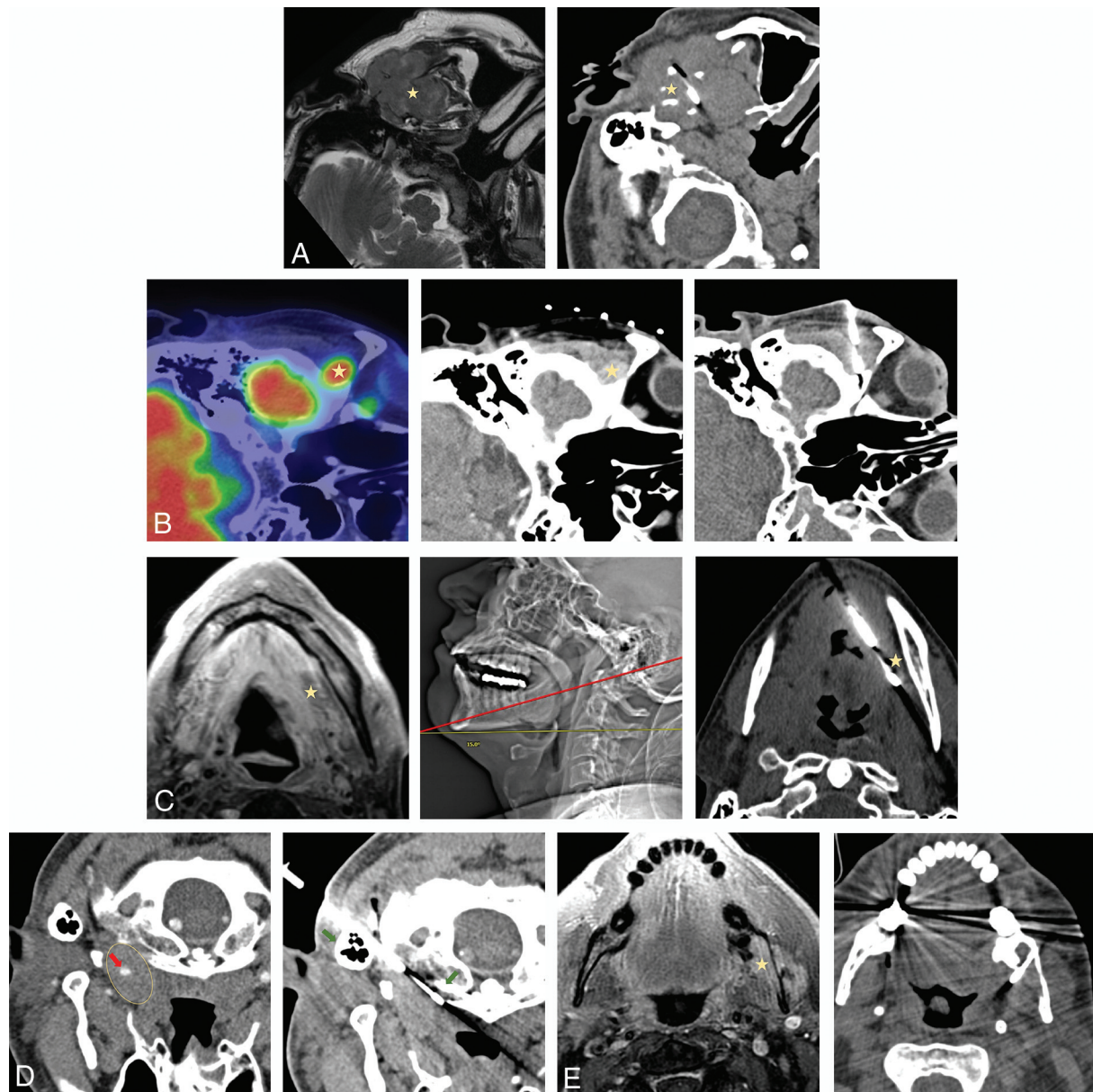


FIG 3. Less commonly used biopsy approaches. **A**, Preauricular approach targeting a 4.2-cm expansile left mandibular lesion with an extraosseous soft-tissue component on MR imaging (left image, yellow star). No preprocedural contrast was administered given the size of the lesion and the lack of proximity of the crucial neurovascular structures. Right, Intraprocedural CT with a 16-ga needle through the lesion. Plasmacytoma. This approach is used for superficial lesions in the masticator or superficial parotid space, particularly when a zygoma is partially destroyed. **B**, A suprazygomatic approach targeting hypermetabolic on PET/CT 1.5-cm right suprazygomatic masticator mass (left image, yellow star). Middle, Preprocedural contrast-enhanced CT (venous phase) to delineate the lesion (yellow star) that enhances more than background tissues. Right, Intraprocedural CT with a 16-ga needle through the expected location of the lesion in correlation with bony landmarks and previous contrast enhancement on the middle image. Recurrent adenoid cystic carcinoma. This approach is essentially exclusively used for superficial suprazygomatic masticator space (temporal fossa) lesions. **C**, Submental approach targeting diffusely heterogeneously enhancing on MR imaging left sublingual/floor of the mouth soft-tissue (left image, yellow star). Middle, Intraprocedural scout CT image showing patient positioning and a cranial gantry tilt of 15° (red line, biopsy plane after 15° gantry tilt) to bypass a mental protuberance. Right, Intraprocedural axial CT with a 14-ga needle through the expected location of the target (yellow star). Preprocedural contrast was not administered due to regional vasculature paucity in correlation with prior imaging. Recurrent adenoid cystic carcinoma. Sublingual space and floor of the mouth lesions can be accessed via this approach; to avoid the mental protuberance, cranial gantry tilt and/or substantial neck extension might be needed. **D**, A retromastoid approach with the patient in the prone position targeting a 2.6-cm left retropharyngeal mass (left image, yellow ellipse), encasing the ICA on preprocedural limited CTA (red arrow). Right, intraprocedural CT with a 16-ga needle advanced between mastoid tip and the C1 anterior arch (right image, green arrows); these osseous landmarks align a safe trajectory into the lesion portion posterior to the ICA in correlation with preprocedural CTA. Recurrent human papillomavirus + SCC. This approach can be used for more lateral retropharyngeal and anterior perivertebral lesions. **E**, A transosseous approach targeting an enhancing 2.5-cm left masticator mass expanding the mandibular canal on MR imaging (left image, yellow star). Right, Intraprocedural CT scan with a 16-ga needle traversing the buccal cortex of the mandibular ramus. Preprocedural contrast was not administered given lack of critical regional vasculature in correlation with MR imaging. Recurrent adenoid cystic carcinoma with inferior alveolar perineural spread. This approach can be used to access lesions along the inner cortex of the mandible and zygoma.

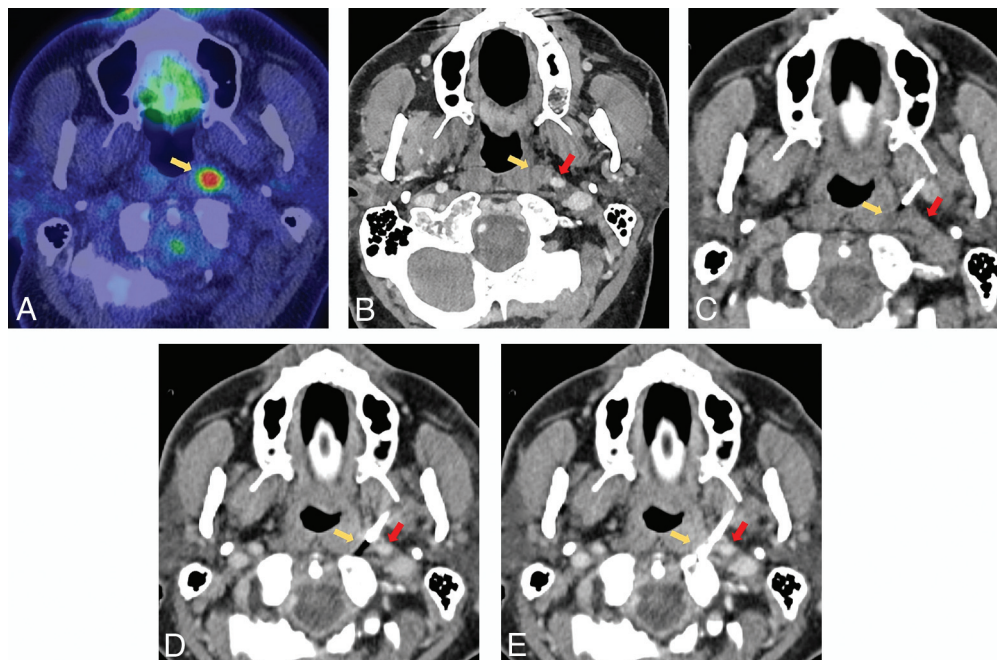


FIG 4. **A,** PET/CT with hypermetabolic left retropharyngeal 6-mm lymph node (yellow arrow). **B,** This lesion is centrally cystic/necrotic on follow-up contrast-enhanced CT (yellow arrow) and immediately medial to the ICA (red arrow). **C,** Intraprocedural CT without contrast with an 18-ga needle advanced via a paramaxillary approach anterior to the target retropharyngeal lymph node (yellow arrow) and medial to the expected location of the unopacified ICA (red arrow). Before further needle advancement, 60 mL of Omnipaque-300 was slowly infused at a rate of 0.6 mL/s to continuously opacify the ICA (red arrows) for adequate visualization before (**D**) and during (**E**) lesion sampling (yellow arrows). Pathology reported poorly differentiated metastatic carcinoma in a patient with a history of oropharyngeal human papillomavirus + SCC.

Table 1: Biopsy approaches

Approach	No.	%
Paramaxillary ^a	43	23%
Retromandibular ^a	30	16%
Anterior ^a	24	13%
Subzygomatic ^a	21	11%
Submandibular ^a	20	11%
Posterior ^a	18	10%
Lateral ^a	14	8%
Preauricular	5	3%
Submental	4	2%
Suprazygomatic	3	2%
Retromastoid	1	1%
Transosseous	1	1%
Total	184	100%

^a More common techniques.

A Temno Evolution core biopsy device (Merit Medical) was used in 167 cases (91%); a Mission Disposable Core Biopsy Device (Bard, BD), in 4 cases (2%); and Stryker Bone Biopsy Kit Needle (Stryker) and SuperCore Semi-Automatic Biopsy Instrument (Argon Medical Devices) were both used in 1 case each. Device type was not specified in 11 cases (6%).

Complications

Minor complications (asymptomatic hematomas) were observed in 4 (2%) cases, none requiring intervention. Manual compression was held for 10–15 minutes, and follow-up CT was performed in the procedure room before the patient was transferred to the postprocedural care unit.

Patient Positioning, Approach, and Intraprocedural Considerations

Patients were positioned supine in 139 (76%), prone in 23 (13%), and in a lateral decubitus position in 22 cases (12%). The H&N position remained relatively neutral in most cases of supine positioning, with the head usually slightly turned to the contralateral side of the lesion.

To optimize access to the target lesion, the gantry was tilted in 14/184 cases (8%). IV contrast was administered for the preprocedural CT in 114/184 cases (62%). While both protocols were used (arterial and venous phase, per proceduralist), the venous phase seemed more optimal, allowing assessment of all 3 major components of the biopsy: target lesion (particularly the solid component in cases of partially cystic/necrotic lesions) and major venous and arterial vasculature, because major arteries are usually still adequately visualized even in the venous phase.

A total of 12 different approaches were used in our cohort, listed in Table 1 along with the number of cases for each approach.

Target Lesion Details

Target lesion size measured in the longest dimension on axial images ranged from 5 to 75 mm (mean, 24 mm). Anatomic spaces of the lesions are summarized in Table 2.

Diagnostic Yield and Histopathologic Biopsy Results

Of 184 core biopsies, 13 were nondiagnostic (7%), with an initial diagnostic yield of 93%. However, of 43/184 (23%) biopsies originally negative for malignancy, 4 were eventually positive for malignancy via

Table 2: Target lesion space

Head and Neck Space	No.	%
Masticator	36	20%
Parotid	24	13%
Cervical lymph nodes ^a	23	13%
Retropharyngeal	23	13%
Sublingual	19	10%
Perivertebral	14	8%
Pharyngeal mucosal	13	7%
Visceral ^b	9	5%
Parapharyngeal	6	3%
Carotid	6	3%
Submandibular	4	2%
Other ^c	4	2%
Transpatial	3	2%
Total	184	100%

^a Cervical lymph node levels II–VI and supraclavicular.

^b Biopsies involving the supraglottic larynx, glottis, subglottic larynx, tracheoesophageal groove, and thyroid gland.

^c Biopsies of the periorbital region, anterior maxilla, preauricular, postauricular, and intramuscular regions.

Table 3: Follow-up of “negative for malignancy” biopsies

Patients' Characteristics and Lesion Management	No.	%
Initially “negative for malignancy” biopsies	43/184	23%
Patients with a known malignancy	29/43	68%
Rebiopsied/excised	7/29	20%
Ultimately + malignancy	4/7	57%
Stable/resolved (mean f/u time: 32 mo, 2–120 mo)	17/29	59%
No f/u	5/29	17%
Patients without known malignancy	14/43	32%
Rebiopsied/excised	5/14	36%
Ultimately + malignancy	0/5	0%
Stable/resolved (mean f/u time: 25.6 mo, 1–72 mo)	7/14	50%
No f/u	2/14	14%
Total false-negative rate	4/184	2%
Total diagnostic yield	167/184	91%

Note:—f/u indicates follow-up.

rebiopsy/surgical excision, resulting in a 2% false-negative rate and an adjusted diagnostic yield of 167/184 (91%). The diagnostic yield was 93% (155/166) for lesions of >10 mm in the greatest axial dimension, but for lesions of ≤10 mm, the yield was only 67% (12/18).

Biopsies were performed by 16 neuroradiologists with variable experience. The diagnostic yield was essentially the same: 91% (64/70) for proceduralists with ≤3 years and 90% (103/114) with >3 years' experience. The diagnostic yield per biopsy needle gauge was as follows: 20 ga, 81% (13/16); 18 ga, 93% (70/75); 16 ga, 90% (64/71), and 14 ga, 91% (20/22). Although we as a practice try to use the largest needle size (smallest gauge) safely possible to get the most tissue, ultimately the choice of the needle gauge was up to the proceduralist, understandably resorting to thinner needles in cases of challenging anatomy (eg, retropharyngeal/carotid/parapharyngeal space and close ICA proximity), but not necessarily in cases of smaller lesions.

Histopathology results are summarized in the Online Supplemental Data. Eighty-six of 184 (47%) lesions were malignant: 23/86 (27%), reflecting primary malignancy; 36/86 (42%), local recurrence; and 27/86 (31%), metastases.

Eighty-five of 184 (46%) lesions were benign, including 43/85 (51%) reported as samples negative for malignancy containing regional tissues.

Of these 43 biopsies initially negative for malignancy, 4/43 (9%) were ultimately positive for malignancy after rebiopsy/excision. Follow-up of biopsies negative for malignancy is summarized in Table 3. Finally, of 13 nondiagnostic biopsies, 3/13 (23%) were ultimately positive for malignancy after rebiopsy/excision.

DISCUSSION

Our study of 184 CT-guided CNBs of H&N lesions represents the largest-to-date single-center retrospective review. This study confirms a very high diagnostic yield of 91% with a low false-negative rate of only 2%. These results in such a large sample with 16 operators with different experience levels are clinically important, suggesting that the described techniques would be generalizable across multiple medical centers. Additionally, on the basis of our large sample size, these procedures are clinically useful because they can be performed safely and efficiently, delivering a timely diagnosis and expediting appropriate treatment while avoiding much more invasive surgical excisional biopsies and with a much higher diagnostic yield than FNAs, especially in cases of unusual etiology.^{2–4,16,17}

Our diagnostic yield of 91%, including a 2% false-negative rate, is concordant with several prior, though much smaller sample studies (each with <30 patients), which showed a diagnostic yield of 73%–100%.^{12–14,18,19}

In addition to being the largest-to-date single-center cohort of CT-guided CNBs of H&N lesions, our study demonstrates a wider variety of biopsy approaches, including transosseous, and provides an extensive morphologic and histologic assessment of 184 lesions. We also describe a novel technique of intraprocedural IV contrast to improve the safety profile through continuous opacification of the adjacent vessels immediately prior to and during lesion sampling in cases of proximity of the vessels to the target lesion.

Our study, in addition to its retrospective design, has a potential limitation of selection bias for lesions that were challenging/inaccessible to excisional or ultrasound-guided biopsy, whether core or FNA. Our institution preferentially performs CT-guided core needle biopsies of H&N lesions as opposed to CT-guided aspiration, with the latter reportedly having up to an 88% concordant diagnostic yield based on the largest study of 216 patients by Sherman et al,¹⁰ in 2004. We also preferentially perform CT-guided CNBs of the superficial H&N lesions as opposed to ultrasound-guided CNB, though Halder et al,⁵ in 2015, reported a very high diagnostic yield (96%) of ultrasound-guided CNB of 313 parotid neoplasms with only 2 samples being false-negatives (versus 44% and 3 samples, respectively, in 120 parotid ultrasound-guided FNAs).

Aiken, in 2020,¹⁷ published a great commentary addressing a practical approach to the triage of H&N biopsies at a major academic institution, which usually starts with FNA and then shifts to core biopsy if directed by the cytopathologist's real-time feedback. We do agree that FNA will usually suffice to diagnose cervical nodal metastasis or recurrence for most

common pathologies such as SCC or thyroid carcinoma, and CNB as opposed to FNA is mostly based on our institutional preference. FNAs are, indeed, often the first step in cases of obvious cervical lymphadenopathy and are not uncommonly performed by our ear, nose, and throat group with ultrasound guidance during the patient encounter. However, cases of impalpable cervical lymphadenopathy and smaller nodes (eg, <1.5 cm) without apparent abnormal morphology on CT would go straight to CT-guided CNB to avoid discrepancies between CT and ultrasound imaging modalities and to maximize the diagnostic yield.

Further prospective studies with high volumes of CT-guided biopsies of H&N lesions could focus on direct comparison of CT-guided core biopsies with FNAs in a variety of anatomic spaces, particularly of more challenging smaller lesions of <10 mm in retropharyngeal and parapharyngeal spaces.

CONCLUSIONS

Our largest-to-date single-center retrospective study of 184 CT-guided core needle biopsies of H&N lesions confirms that these procedures can be performed safely with a high diagnostic yield by operators with variable experience. In addition to gantry tilt and preprocedural IV contrast administration for vessel and target lesion mapping, continuous intraprocedural IV contrast infusion during lesion sampling can significantly facilitate the procedure and increase the safety profile.

Disclosure forms provided by the authors are available with the full text and PDF of this article at www.ajnr.org.

REFERENCES

1. Siegel RL, Miller KD, Fuchs HE, et al. **Cancer statistics, 2021.** *CA A Cancer J Clin* 2021;71:7–33 [CrossRef Medline](#)
2. Huang YC, Wu CT, Lin G, et al. **Comparison of ultrasonographically guided fine-needle aspiration and core needle biopsy in the diagnosis of parotid masses.** *J Clin Ultrasound* 2012;40:189–94 [CrossRef Medline](#)
3. Song IH, Song JS, Sung CO, et al. **Accuracy of core needle biopsy versus fine needle aspiration cytology for diagnosing salivary gland tumors.** *J Pathol Transl Med* 2015;49:136–43 [CrossRef Medline](#)
4. Ryu YJ, Cha W, Jeong J, et al. **Diagnostic role of core needle biopsy in cervical lymphadenopathy.** *Head Neck* 2015;37:229–33 [CrossRef Medline](#)
5. Halder S, Mandalia U, Skelton E, et al. **Diagnostic investigation of parotid neoplasms: a 16-year experience of freehand fine needle aspiration cytology and ultrasound-guided core needle biopsy.** *Int J Oral Maxillofac Surg* 2015;44:151–57 [CrossRef Medline](#)
6. Drylewicz MR, Watkins MP, Shetty AS, et al. **Formulating a treatment plan in suspected lymphoma: ultrasound-guided core needle biopsy versus core needle biopsy and fine-needle aspiration of peripheral lymph nodes.** *J Ultrasound Med* 2019;38:581–86 [CrossRef Medline](#)
7. Abrahams JJ. **Mandibular sigmoid notch: a window for CT-guided biopsies of lesions in the parapharyngeal and skull base regions.** *Radiology* 1998;208:695–99 [CrossRef Medline](#)
8. Gupta S, Henningsen JA, Wallace MJ, et al. **Percutaneous biopsy of head and neck lesions with CT guidance: various approaches and relevant anatomic and technical considerations.** *Radiographics* 2007;27:371–90 [CrossRef Medline](#)
9. McKnight CD, Glastonbury CM, Ibrahim M, et al. **Techniques and approaches for safe, high-yield CT-guided suprahyoid head and neck biopsies.** *AJR Am J Roentgenol* 2017;208:76–83 [CrossRef Medline](#)
10. Sherman PM, Yousem DM, Loevner LA. **CT-guided aspirations in the head and neck: assessment of the first 216 cases.** *AJNR Am J Neuroradiol* 2004;25:1603–07 [Medline](#)
11. Tu AS, Geyer CA, Mancall AC, et al. **The buccal space: a doorway for percutaneous CT-guided biopsy of the parapharyngeal region.** *AJNR Am J Neuroradiol* 1998;19:728–31 [Medline](#)
12. Connor SEJ, Chaudhary N. **CT-guided percutaneous core biopsy of deep face and skull-base lesions.** *Clin Radiol* 2008;63:986–94 [CrossRef Medline](#)
13. Wu EH, Chen YL, Wu YM, et al. **CT-guided core needle biopsy of deep suprahyoid head and neck lesions.** *Korean J Radiol* 2013;14:299–306 [CrossRef Medline](#)
14. Hillen TJ, Baker JC, Long JR, et al. **Percutaneous CT-guided core needle biopsies of head and neck masses: technique, histopathologic yield, and safety at a single academic institution.** *AJNR Am J Neuroradiol* 2020;41:2117–22 [CrossRef Medline](#)
15. Grewal A, Khera SS, McGahan JP, et al. **Utility of intra-procedural contrast enhanced CT in ablation of renal masses.** *AJR Am J Roentgenol* 2020;214:122–28 [CrossRef Medline](#)
16. Park YM, Oh KH, Cho JG, et al. **Analysis of efficacy and safety of core-needle biopsy versus fine-needle aspiration cytology in patients with cervical lymphadenopathy and salivary gland tumour.** *Int J Oral Maxillofac Surg* 2018;47:1229–35 [CrossRef Medline](#)
17. Aiken AH. **Image-guided biopsies in the head and neck: practical value and approach.** *AJNR Am J Neuroradiol* 2020;41:2123–25 [CrossRef Medline](#)
18. Wu EH, Chen YL, Toh CH, et al. **CT-guided core needle biopsy of deep suprahyoid head and neck lesions in untreated patients.** *Interv Neuroradiol* 2013;19:365–69 [CrossRef Medline](#)
19. Cunningham JD, McCusker MW, Power S, et al. **Accessible or inaccessible? Diagnostic efficacy of CT-guided core biopsies of head and neck masses.** *Cardiovasc Intervent Radiol* 2015;38:422–29 [CrossRef Medline](#)